Turkish Journal of Chemistry

Volume 39 | Number 2 Article 2

1-1-2015

A green light emitting polymer in a PMMA matrix: oligo(azomethine-ether) with benzothiazole moieties

MEHMET YILDIRIM

İSMET KAYA

Turkish Journal of Chemistry

http://journals.tubitak.gov.tr/chem/

Research Article

Turk J Chem
(2015) 39: 217 – 234

doi:10.3906/kim-1405-66

A green light emitting polymer in a PMMA matrix: oligo(azomethine-ether) with benzothiazole moieties

Mehmet YILDIRIM[1,2], **İsmet KAYA**[1,*]
[1]Polymer Synthesis and Analysis Laboratory, Department of Chemistry, Faculty of Science and Arts, Çanakkale Onsekiz Mart University, Çanakkale, Turkey
[2]Department of Materials Science and Engineering, Faculty of Engineering, Çanakkale Onsekiz Mart University, Çanakkale, Turkey

Received: 23.05.2014 • **Accepted/Published Online:** 24.08.2014 • **Printed:** 30.04.2015

Abstract: This study aimed to synthesize an oligo(azomethine-ether) with benzothiazole moiety in organic medium by means of chemical oxidative polycondensation (OP). Optical properties were examined by photoluminescence (PL) and UV-Vis measurements both in solutions and solid film involved a poly (methyl methacrylate) (PMMA) matrix. Oligomer film in the PMMA matrix emitted a fine green light with a fluorescence quantum yield (QY) of 3.30%. Spectral and thermal observations showed a high rate of C–O–C coupling (cross-linking) for the oligomer. SEC results indicated low molecular weight ($\sim$3200–4650 g mol^{-1}) and the oligomer was soluble in organic solvents with high polarity. Electrochemical behavior was characterized by cyclic voltammetry (CV), morphological properties by scanning electron microscopy (SEM), and thermal characteristics by TG-DTA and DSC techniques.

Key words: PLED, green emission, cross-linking, conjugated polymers, oligo(azomethine-ether)

1. Introduction

Conjugated polymers with aromatic backbones have been used in several application fields due to their superior properties.[1] Aromatic backbones have given high thermal stability to polymers. Some aromatic dianhydride based polymers exhibited fine flame retardancy properties as well.[2] Furthermore, polyconjugated structures have brought low band gaps, resulting in good electrical and optical properties. However, polymers with aromatic structures generally suffer from low solubility in common solvents, and thus their processibility is limited.

Conjugated polymers are used in polymeric light emitting diodes (PLEDs),[3–6] electrochromic materials,[7,8] electronic and opto-electronic devices,[9] and gas and ion sensors.[10,11] Poly(azomethine)s[12] and poly(phenol)s[13] are important classes of conjugated polymers. Phenol based monomers are able to be oxidized into phenoxy radical in appropriate conditions.[14] Several kinds of initiators could be used in OP reactions like NaOCl, organic and inorganic peroxides, and air oxygen.[15] Reactions can be catalyzed by a peroxidase based enzyme such as horseradish peroxidase (HRP).[16] Both organic and aqueous solutions can be used in such a polymerization reaction. Furthermore, electrochemical oxidation is used for polymerization. OP reactions of phenol based monomers often produce both phenoxy and phenylene radicals together.[17] These kinds of radicals form polymer chains by C–C or C–O–C coupling. As the polymerization predominantly proceeds by C–C coupling

*Correspondence: kayaismet@hotmail.com

free hydroxyl groups are found in the resulting polymer's structure. If the C–O–C coupling mainly forms in the polymer chain, the number of free hydroxyl groups decreases and the polymer is called a poly(ether). These different linkages significantly affect the thermal degradation behavior of polymers.[18] Chain breaking at the phenylene linkage (C–C coupled) generally occurs at about 300 °C and the etheric linkage is observed over 700 °C. That is to say, a high rate of C–O–C etheric linkage results in the formation of a more stable structure. To increase the C–O–C coupling rate, structural modifications over the previously synthesized poly(azomethine-phenol)s could be useful. Among the hydroxyphenylene substituted Schiff base monomers the species derived from 4-hydroxybenzaldehyde are more suitable for C–O–C coupling (lower steric hindrance) in OP conditions. Therefore, they can be chosen to obtain a higher thermal stability.[19] On the other hand, to overcome the insolubility problem of the obtained branched-chain structured polymer,[20] mild conditions might be preferred, producing oligomers with a lower molecular weight[21] and greater solubility.[17]

Cross-linking in a polymer structure is a kind of limitation for the individual chain movement and results in a higher rigidity, as well as decreasing the solubility. However, it becomes more resistant to thermal degradation. Several kinds of poly(ether)s with cross-linked structures have been synthesized so far.[22–24] They have shown good thermal and mechanical properties, but generally they have been insoluble in common organic solvents, because cross-linked polymers often swell in solvents instead of solvation.

The goal of this study was to prepare a highly stable, organo-soluble, low molecular weight oligomer having high fluorescence characteristics. For that purpose, we synthesized a new kind of cross-linked oligo(ether) including a phenylene-benzothiazole based backbone by a chemical OP reaction. An ethoxy substituted benzothiazole compound was chosen to increase solubility. According to the previous studies, OP reactions in organic solvents produced highly soluble products having higher crystallinity, well-ordered particles, and fine fluorescence characteristics as compared with their production in aqueous alkaline medium.[20,25] For this reason, the results obtained in organic reaction medium are given here. OP of the monomer was also carried out in aqueous alkaline medium and the product was fully analyzed. However, the results were unsatisfactory and are not included in this study. The optical properties of the materials were studied in both solution form and film state involved in a PMMA matrix. Polymer matrices have been preferred in many studies to produce fluorescence based sensing probes for heavy metal ions,[26] electrochromic device preparation[27] etc. This kind of application supplies more useful information about how the produced material can be applied in practice usage, because LEDs and many other optical devices require the material to be used in solid state. This can be supplied by treatment with an appropriate matrix component like poly(methyl methactrylate), ethyl cellulose, and poly (vinyl chloride). The electrochemical, morphological, and thermal properties of the materials were also clarified.

2. Results and discussion

2.1. Structures of the synthesized compounds

4-HBAEBT and its oligomer have yellow needle-like crystalline particles and black powder form particles, respectively. Both of them are soluble in strong polar organic solvents like DMF and DMSO. 4-HBAEBT is also soluble in other polar solvents such as MeCN, MeOH, THF, and $CHCl_3$ while insoluble in nonpolar solvents such as toluene, n-hexane, and 1,4-dioxane. O-4-HBAEBT is partially soluble in THF, MeOH, and $CHCl_3$, but is insoluble in the other solvents used.

According to the SEC results bimodal peaks are obtained, indicating that O-4-HBAEBT has two particular fractions. M_n, M_w, PDI and % values of the first and second fractions are 6800, 8900 g mol^{-1},

1.32, and 37%; and 1100, 2350 g mol^{-1}, 2.15, and 63%, respectively. Totally, the oligomer has a number average molecular weight (M_n) of about 3210 g mol^{-1}. On the other hand, homopolymers of unsubstituted 2-amino-6-ethoxybenzothiazole (P-EBT), which were previously synthesized by OP[20] and electropolymerization methods,[28] had higher molecular weights (M_n values were approximately 15,000 and 300,000 g mol^{-1}, respectively) than the iminophenylene substituted one synthesized here.

FT-IR spectra of the starting materials, 4-HBAEBT and O-4-HBAEBT, are given in Figures 1a and 1b, respectively. The first glance at the spectrum of the Schiff base (Figure 1a) shows that the structure is confirmed by disappearance of the C=O (carbonyl) stretching vibration of 4-HBA at 1663 cm^{-1} and the N–H stretching vibration of EBT at 3417–3434 cm^{-1}. A new peak indicating the C=N stretching of the imine bond is observed at 1596 cm^{-1}. This peak shifts to 1638 cm^{-1} in the spectrum of the oligomer. After the polymerization, broad absorption peaks are observed. This is because of the polyconjugated structure of the oligomer.[17] O–H and aliphatic C–H stretching bands are also observed at 3360 and 2977 cm^{-1} in the spectrum of the oligomer, respectively. On the other hand, there is no particular O–H band over 3000 cm^{-1} in the spectrum of 4-HBAEBT. However, a weak and broad peak ranging in a large scale of about 3000–2600 cm^{-1} is attributed to intermolecular hydrogen bonded phenolic –OH.

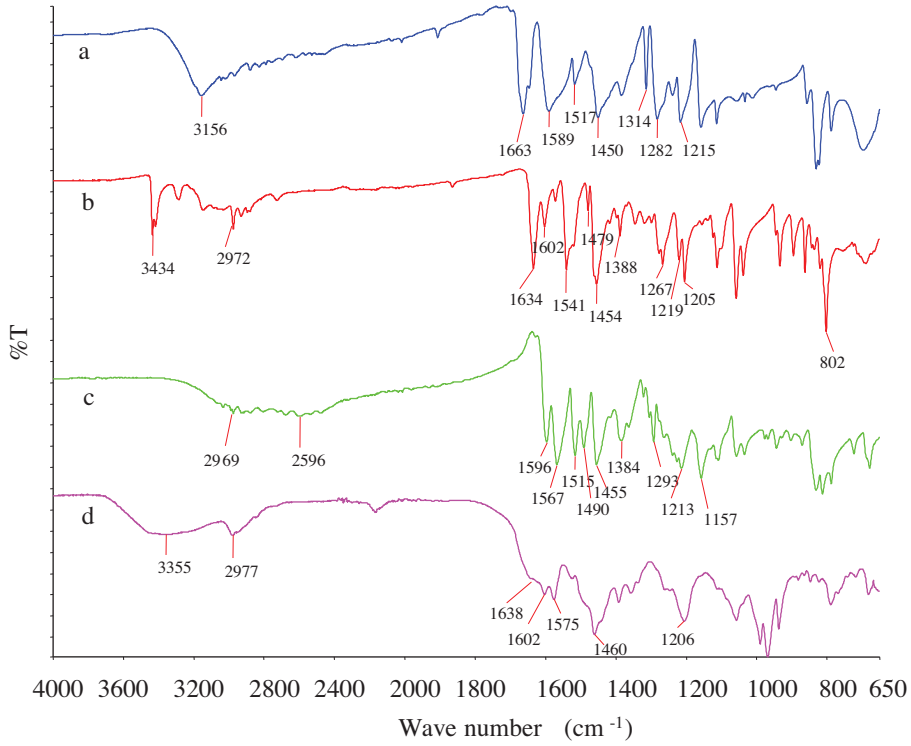

Figure 1. FT-IR spectra of 4-HBA (a), EBT (b), 4-HBAEBT (c), and O-4-HBAEBT (d).

The ^{1}H NMR spectra of 4-HBAEBT and O-4-HBAEBT are shown in Figures 2a and 2b, respectively. The peak integrations of 4-HBAEBT (shown on the spectrum) clearly confirm the Schiff base formation. According to the spectra, imine (HC=N) protons are observed at 8.98 and 9.61 ppm for 4-HBAEBT and O-4-HBAEBT, respectively. A –OH signal of 4-HBAEBT is clearly observed at 10.58 ppm, but no particular –OH band is observed for the oligomer. This indicates a high rate of C–O–C coupling in the polymerization.[17] In the

spectrum of the oligomer the peaks belonging to Ha and Hc protons completely disappear, indicating C–C coupling by elimination of Ha and Hc protons. As a result, the polymerization proceeds on both sides of the Schiff base (the sides of benzothiazole and phenol). The possible polymerization mechanism of 4-HBAEBT including both C–C and C–O–C couplings is suggested in Scheme 1 similar to the other oligophenols in the literature.[16,17] According to the OP mechanism of phenolic monomers, the reaction starts by oxidation of phenolic OH, which converts to a phenoxy radical form by oxidant addition (see Scheme 1). This radical might be transferred into the benzothiazole by movements of delocalized π-conjugated electrons. As a result, a series of possible resonance forms of 4-HBAEBT are obtained as shown in Scheme 2. The obtained spectral findings show that R1, R2, and R6 radicals are the active species contributed to the polymerization. Therefore, the polymerization proceeds on both the benzothiazole and phenol sides, as indicated for similar structures.[20]

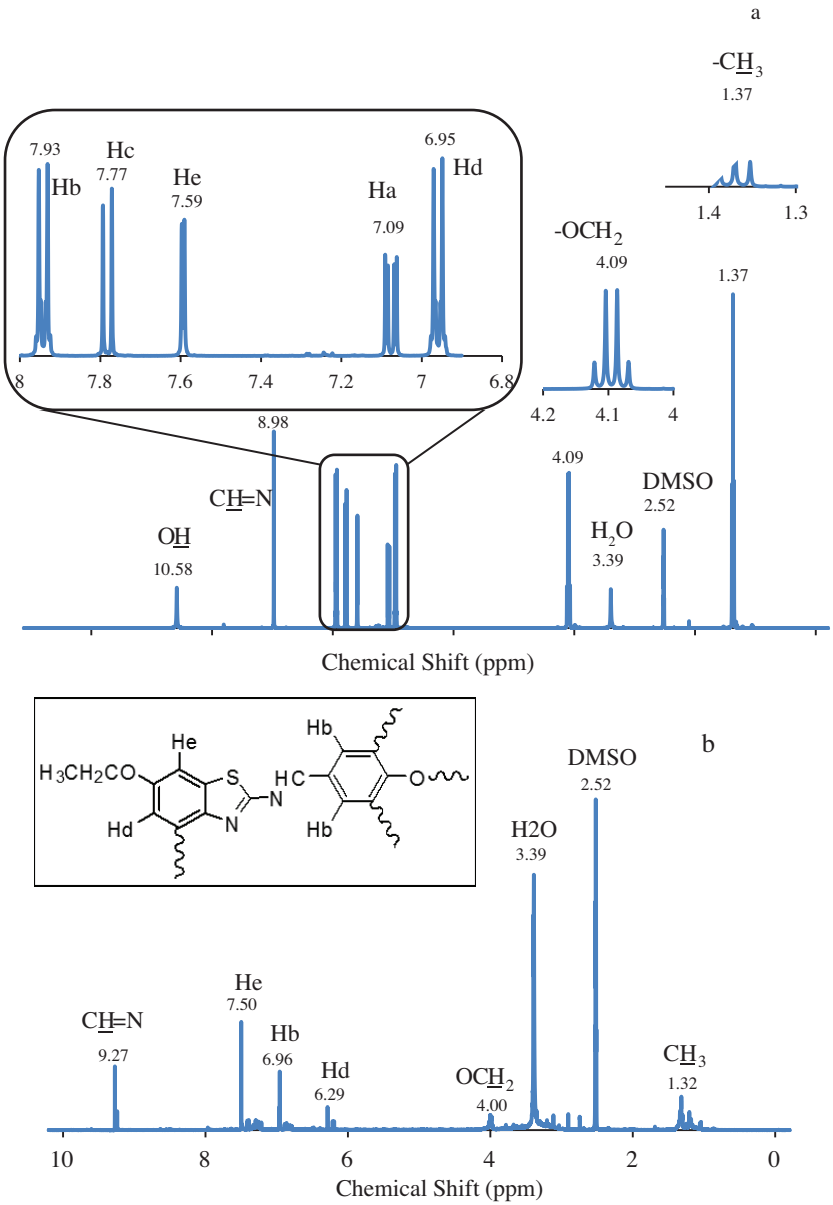

Figure 2. ^{1}H NMR spectra of 4-HBAEBT (a) and O-4-HBAEBT (b).

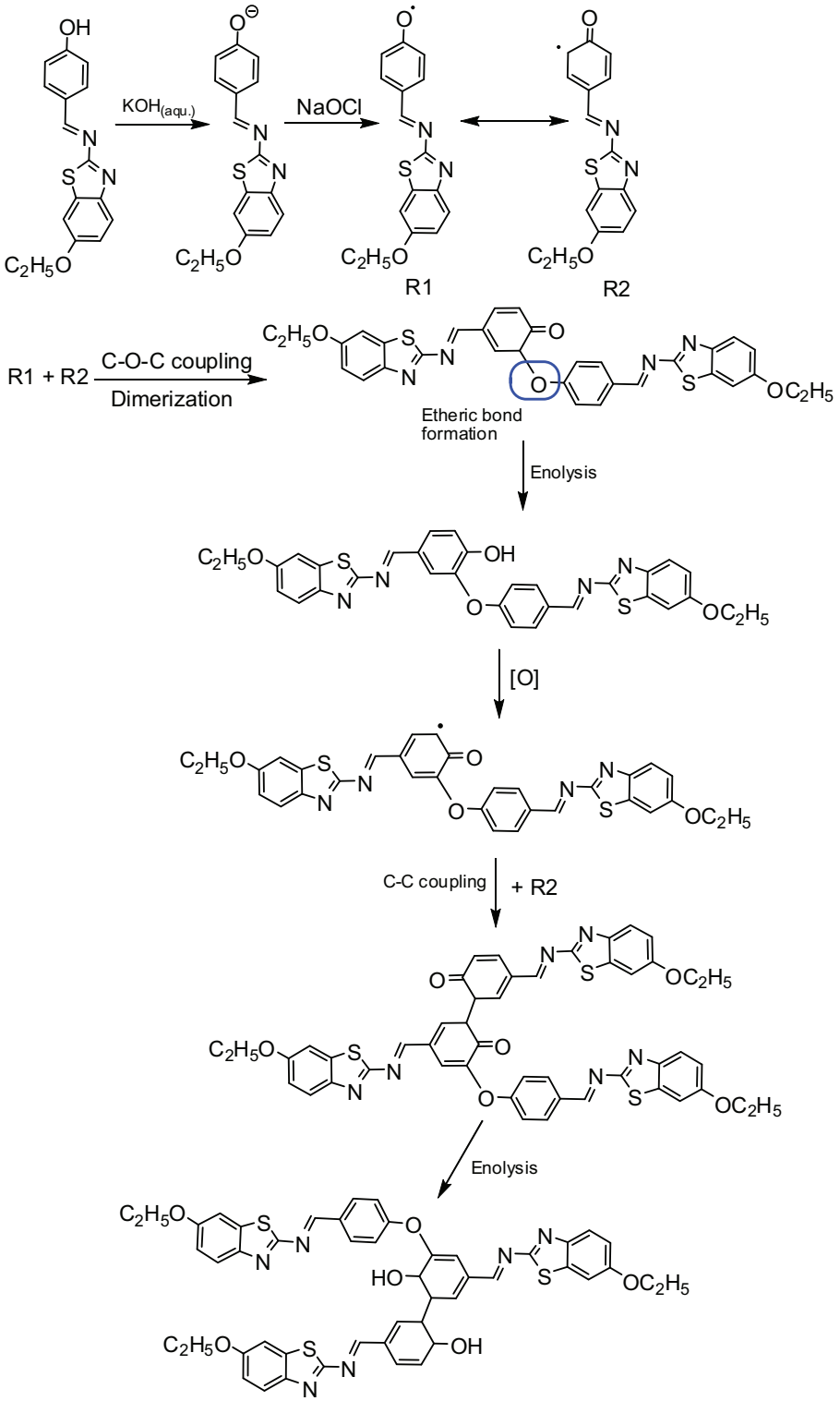

Scheme 1. Possible polymerization mechanism of 4-HBAEBT including C–O–C and C–C coupling.

The ^{13}C NMR of 4-HBAEBT is shown in Figure 3. The obtained signals confirm the expected structure. According to the spectrum there are fourteen different peaks in accordance with the structure. ^{13}C NMR

analysis of the oligomer is also carried out, but no determinable peaks are obtained due to its relatively low solubility.

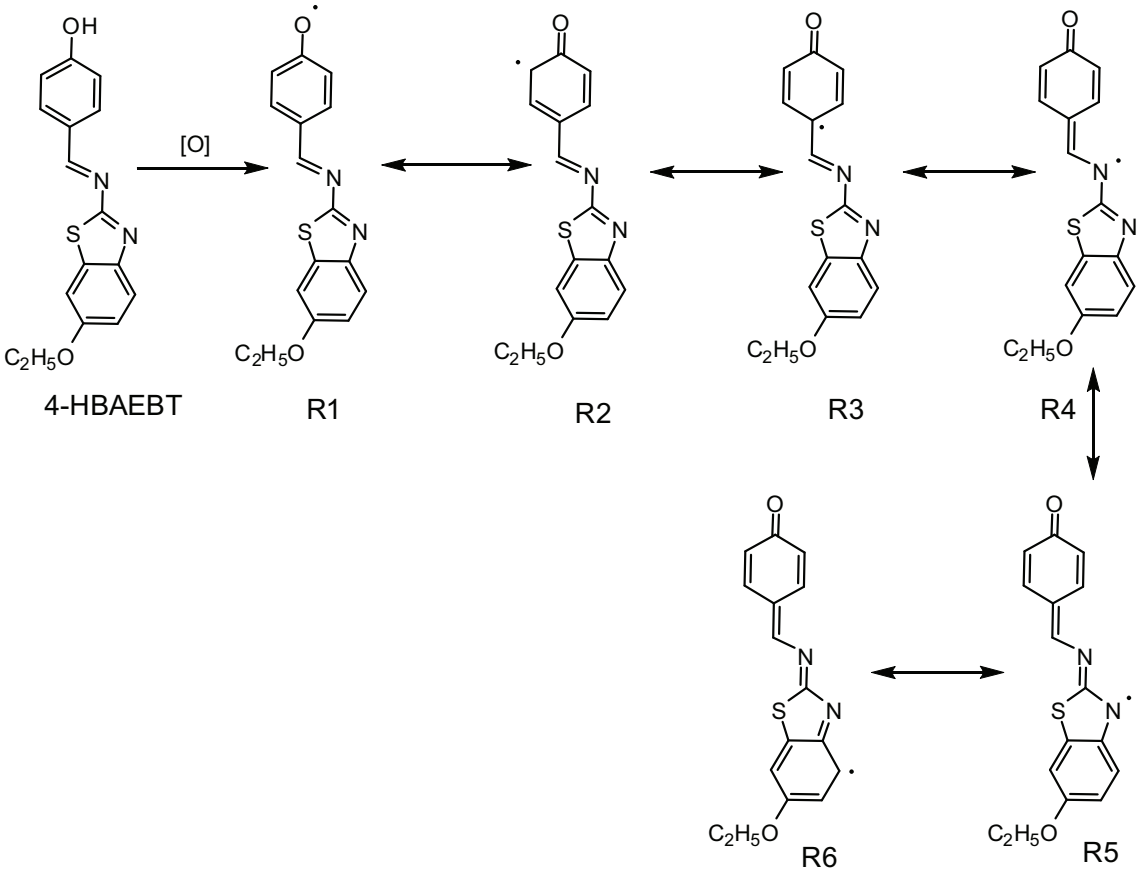

Scheme 2. Radicalic resonance forms of 4-HBAEBT.

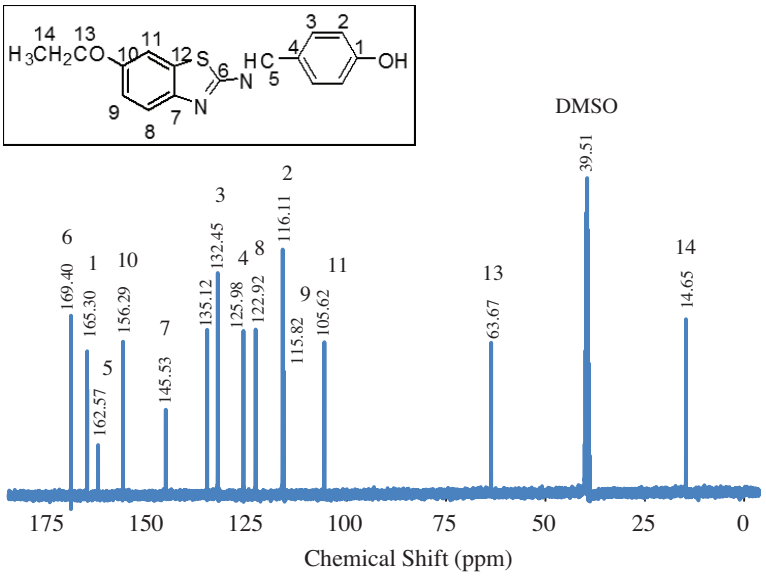

Figure 3. ^{13}C NMR spectrum of 4-HBAEBT.

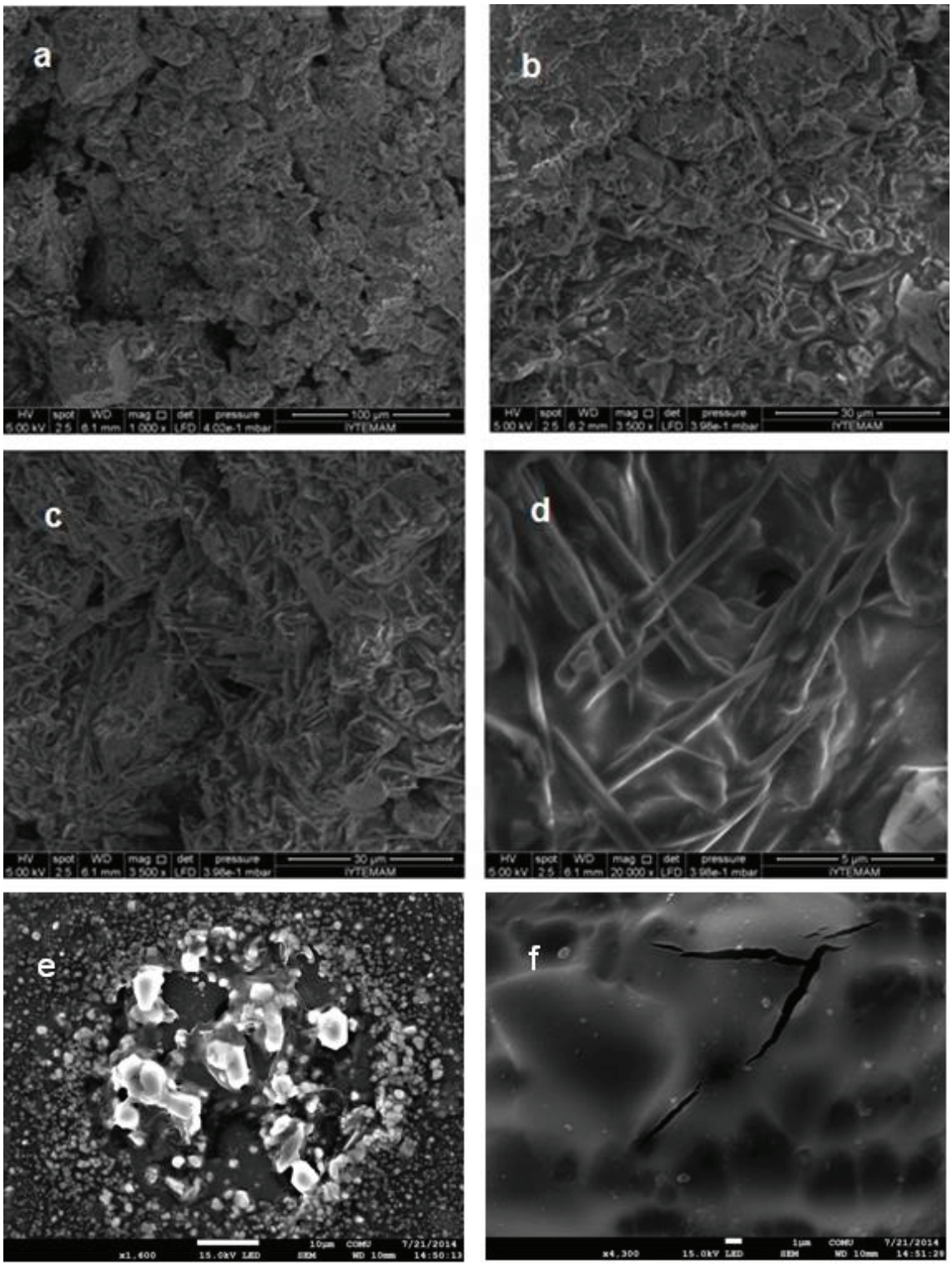

Figure 4. SEM images of O-4-HBAEBT in powder form (a–d) and in PMMA matrix (e and f).

SEM images of O-4-HBAEBT powder with various magnifications are shown in Figures 4a–4d. Figure 4a, with a scale of 100 μm, shows a rocky-like view with certain hollows. On the other hand, in the magnified

picture in Figure 4d, with a scale of 5 μm, a very interesting morphology with icicle-like particles is observed. SEM images of O-4-HBAEBT in the PMMA matrix (film material) are also given in Figures 4e and 4f. As seen in these images, due to the presence of a few components in the gel matrix, an inhomogeneous morphology is observed. Moreover, Figure 4f shows that the obtained film contains some local micro fractures, as well.

2.2. Optical and electrochemical behavior

The UV-Vis spectra of EBT and the synthesized materials are given in Figure 5A. The normalized absorption spectra of 4-HBAEBT and O-4HBAEBT ranging from 380 to 600 nm are given in Figure 5B to make the absorption edges more visible. Both the starting materials and the resulting products show a $\pi \rightarrow \pi^*$ transition of the phenylene ring at $\sim$220 nm. The spectrum of EBT has an absorption peak (λ_{max}) at 267 nm, which indicates that the n$\rightarrow \pi^*$ electronic transitions belong to the amine group. The absorption spectrum of 4-HBAEBT differs from that of the starting materials by a new peak at 377 nm. This new peak is attributed to n$\rightarrow \pi^*$ transition of the azomethine group. The λ_{max} value of O-4-HBAEBT is 336 nm and lower than that of 4-HBAEBT. However, as seen in Figure 5B the oligomer has an absorption tail, indicating a red shifted absorption edge. The optical band gaps (E_g^{opt}) of 4-HBAEBT and O-4-HBAEBT are found as 2.76 and 2.47 eV, respectively. The lower band gap of the oligomer arises from its polyconjugated structure.

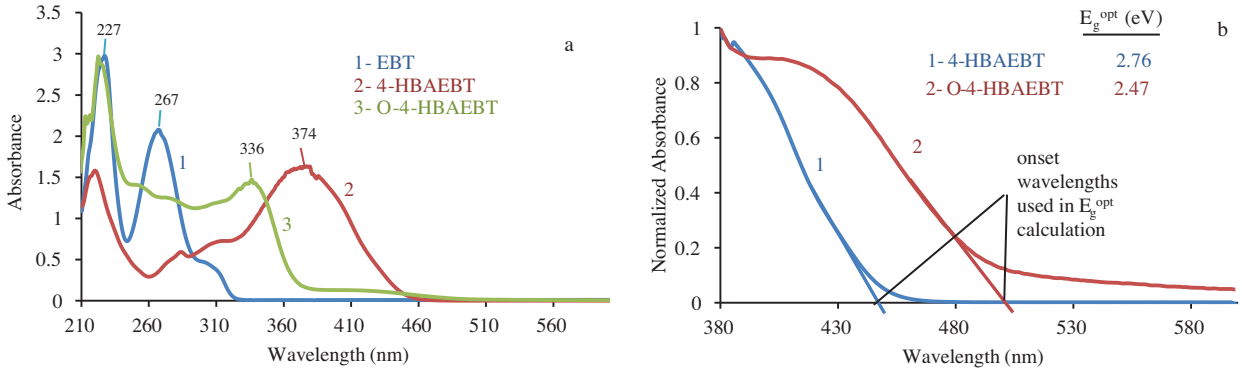

Figure 5. UV-Vis spectra of EBT, 4-HBAEBT, and O-4-HBAEBT solutions in MeOH (A) and normalized absorption spectra of 4-HBAEBT (1) and O-4-HBAEBT (2) in MeOH solutions (B).

PL analyses of the synthesized materials are carried out in $CHCl_3$ and DMF solutions in order to determine the effect of solvent polarity on PL properties. However, there is no determinable signal in the PL spectrum of 4-HBAEBT in $CHCl_3$ solution. 4-HBAEBT gives a low signal in DMF solution, indicating lower fluorescence quantum yield, but O-4-HBAEBT has good fluorescence characteristics in both solutions. The normalized PL spectra of the monomer and O-4-HBAEBT are given in Figure 6. The fluorescence data are also summarized in Table 1. DMF solution of O-4-HBAEBT has a 5 nm red shifted (515 nm) and wider emission band than that of the monomer. Furthermore, the emission peak wavelength of O-4-HBAEBT in DMF solution is about 95 nm red shifted than that in $CHCl_3$ solution (420 nm). This is attributed to the solvent polarity difference.[16] Emission maxima of the oligomer in the solvents with high polarities are higher than those with low polarities. 4-HBAEBT emits blue and green light in $CHCl_3$ and DMF solutions, respectively. Stokes' losses ($\Delta(h\upsilon)_{ST}$) are 0.26 eV for 4-HBAEBT in DMF, 0.29 eV for O-4-HBAEBT in DMF, and 0.73 eV for O-4-HBAEBT in $CHCl_3$. Stokes' loss is defined in the *Oxford Dictionary of Biochemistry* as the loss of excitation energy available for fluorescence due to collision of molecules with their neighbors in the first excited

state, S_2. This results in a lower vibration level of S_1. As a result, loss of applied energy for O-4-HBAEBT is approximately 2.5 times lower in DMF solution than that in $CHCl_3$. According to Table 1, the absorbed photon energy needed for fluorescence, $(h\upsilon)_A$, is also lower in DMF solution for O-4-HBAEBT (2.70 eV). Stokes' loss percentages are accordingly 19.8% and 10.7% for $CHCl_3$ and DMF solutions, respectively, which are calculated as the ratio of $\Delta(h\upsilon)_{ST}/(h\upsilon)_A$. Resultantly, due to lower energy extravagance DMF solution of O-4-HBAEBT could be preferred for fluorescence. On the other hand, full width of half maximum (FWHM) values of O-4-HBAEBT in $CHCl_3$ and DMF are calculated as 0.56 and 0.33 eV, respectively. This means that the FWHM value of O-4-HBAEBT in DMF is smaller than that in $CHCl_3$, and thus the emitted light from the DMF solution is more monochromatic.

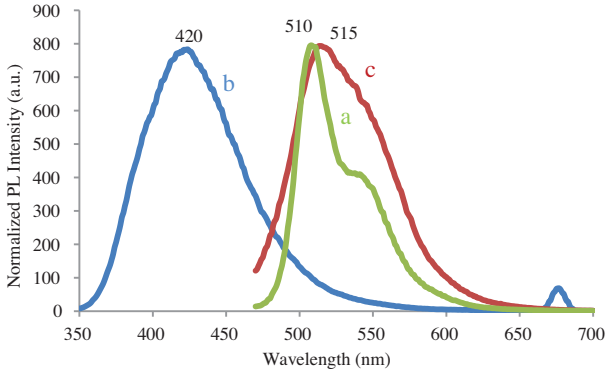

Figure 6. Normalized PL spectra of 4-HBAEBT in DMF (a, λ_{Ex} 460 nm), O-4-HBAEBT in $CHCl_3$ (b, λ_{Ex} 336 nm), and O-4-HBAEBT in DMF (c, λ_{Ex} 460 nm). Slit width: 5 nm.

Table 1. Fluorescence related data of the solutions of synthesized materials.

Materials	λ_{Ex} (nm)	λ_{Em} (nm)	$(h\upsilon)_A$ (eV)	$(h\upsilon)_F$ (eV)	$\Delta(h\upsilon)_{ST}$ (eV)	FWHM (eV)
4-HBAEBT[a]	460	510	2.70	2.44	0.26	0.22
O-4-HBAEBT[a]	460	515	2.70	2.41	0.29	0.33
O-4-HBAEBT[b]	336	420	3.69	2.96	0.73	0.56

Solvent: [a] DMF [b] $CHCl_3$

Electrochemical oxidation/reduction behavior of the synthesized materials is investigated by CV analyses. Cyclic voltammograms obtained on a glassy carbon electrode (GCE) under argon atmosphere are given in Figure 7. The CV data are summarized in Table 2. The observed oxidation peaks probably arise from the oxidation of free –OH groups to form phenoxy radicals ($PhO^{\cdot}$), as indicated in the literature,[19] and relatively low current intensity indicates the low rate of free OH groups in the oligomer structure. The reduction peaks observed are most probably due to the reduction of the imine bonds via protonation of imine nitrogen (C=N–). There are two imine nitrogens available for this reduction process: imine between thiazole and phenylene rings (this group is formed after the Schiff base reaction) and imine in the thiazole ring. According to the CV analysis results, the electrochemical band gaps (E'_g) of 4-HBAEBT and O-4-HBAEBT are calculated as 2.75 and 1.64 eV, respectively. Electrochemical HOMO–LUMO and E'g energy diagram is also illustrated and given in Figure 7. Accordingly, an increase in LUMO level and a decrease in HOMO level are observed, which cause a lower band gap of the oligomer.

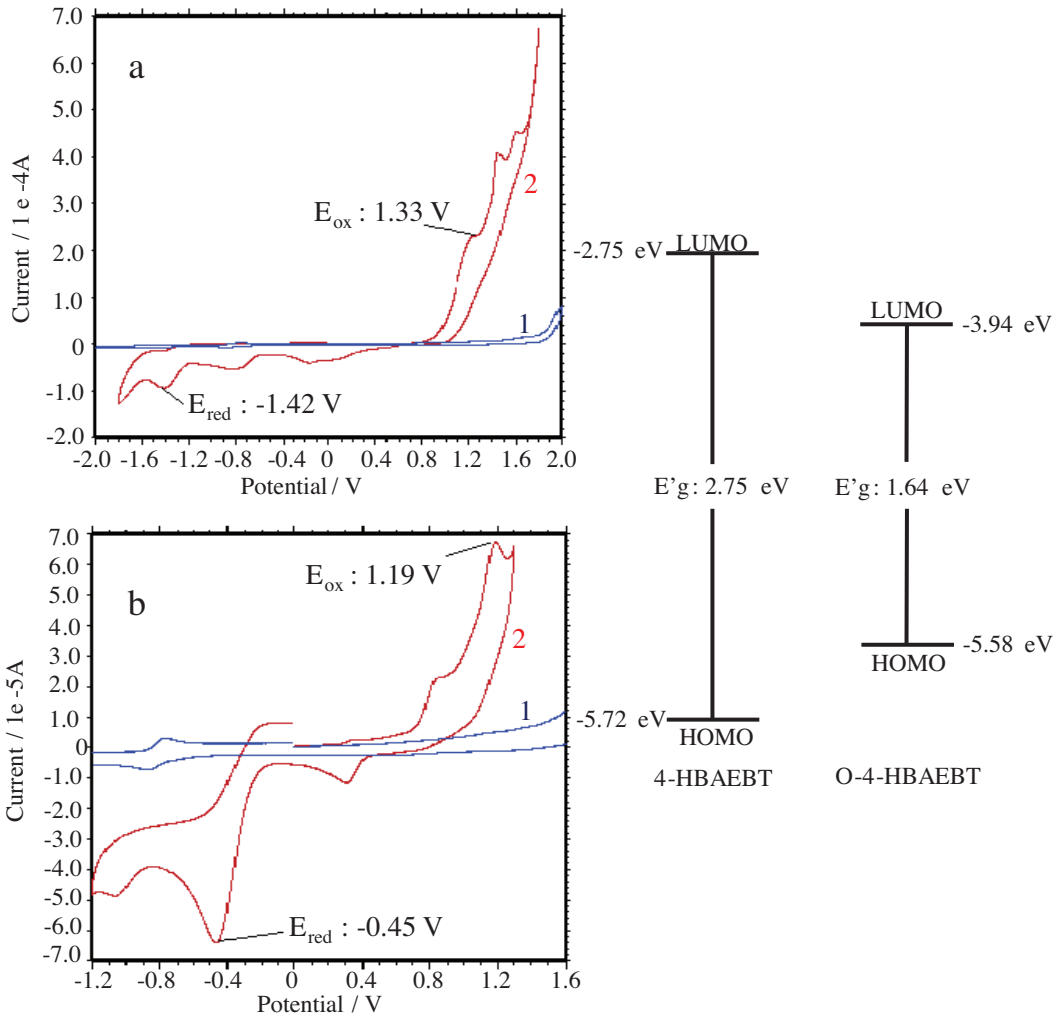

Figure 7. Left side: Cyclic voltammograms of 4-HBAEBT (a-2) and O-4-HBAEBT (b-2) on GCE working electrode in MeCN/DMSO (4/1, v/v) solvent mixtures (blank was given as 1 on the voltammograms). Scan rate: 200 mV s^{-1}, supporting electrolyte: $TBAPF_6$. Conc. of the materials: 0.1 g L^{-1}. Right side: Electrochemical energy diagram illustrated using the CVs.

Table 2. CV analysis results.

Materials	E_{ox} (eV)	$E_{red}(1)$ (eV)	HOMO	LUMO	E'_g (eV)
4-HBAEBT	1.33	–1.42	–5.72	–2.97	2.75
O-4-HBAEBT	1.19	–0.45	–5.58	–3.94	1.64

2.3. Optical characteristics in the PMMA matrix

Solid state optical properties of 4-HBAEBT and O-4-HBAEBT are also investigated in the PMMA gel matrix. Film colors of 4-HBAEBT and O-4-HBAEBT deposited onto transparent polyester surface are yellow and light brown under sunlight, respectively (see Figure 8 - top side). PL spectra on the film surfaces are shown in Figure 8. Emitted color photographs under excitation of 340 nm are also shown on the spectra. According to the obtained results 4-HBAEBT and its oligomer emit blue and green light, respectively. Emission maxima

of the monomer and oligomer are 494 and 533 nm. O-4-HBAEBT in the PMMA matrix has an 18 nm red shifted emission maximum compared to that in DMF solution. On the other hand, QY of the oligomer and the monomer in the PMMA matrix is calculated as 3.30% and 0.06%, respectively. This indicates that the oligomer has about 50 times higher QY than the monomer. QY is an important term in fluorescence properties and higher QY indicates a strong emission color. Resultantly, the synthesized oligomer emits a green color with high intensity in the PMMA matrix. QY, however, is related to various factors used such as concentration of the oligomer used in the PMMA matrix and film thickness. QY of the material can be increased by changing these important values, and so the material can be more useful for light emitting applications.

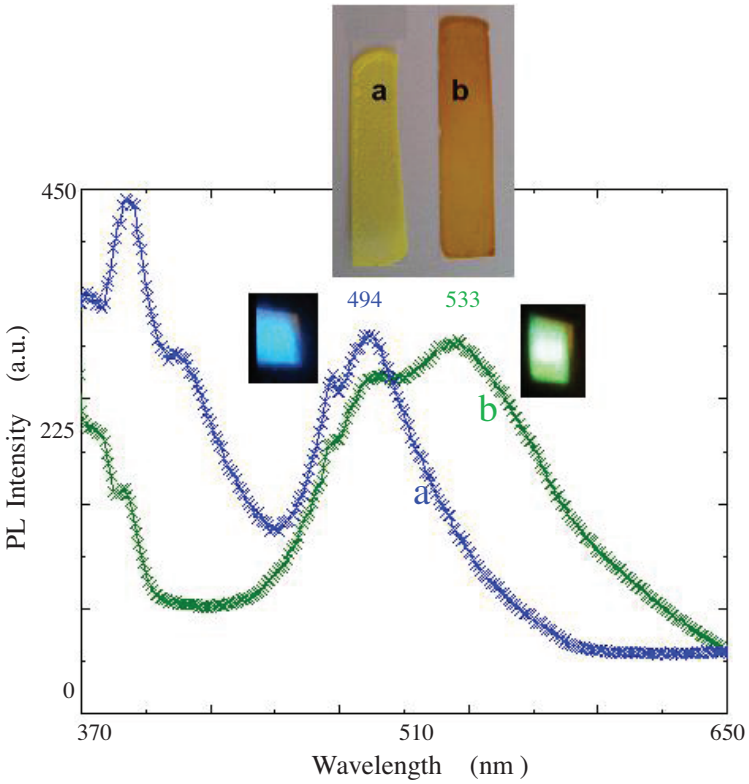

Figure 8. PL spectra of 4-HBAEBT (a) and O-4-HBAEBT (b) homogeneous films on transparent polyester plate prepared from PMMA gel matrix and the emission colors on the spectra. λ_{Ex}: 340 nm. Inserted photographs (top) are taken under sunlight.

Absorption spectra of the materials in the PMMA matrix are given in Figure 9. The optical band gaps of 4-HBEBT and O-4-HBAEBT in the PMMA matrix are calculated from the absorption edges as 2.57 and 2.10 eV, respectively. Resultantly, the materials in the PMMA matrix have lower band gaps as well as red shifted PL peaks.

2.4. Thermal characterization

Thermal degradation characteristics of 4-HBAEBT and its oligomer are determined by TG-DTA method and the data are summarized in Table 3. The obtained TG-DTA curves are given in Figure 10. Both of the materials decompose in two particular steps. The onset degradation temperature (T_{on}) of the monomer is 249 °C, while that of O-4-HBAEBT is 293 °C. This indicates that the synthesized oligomer is more stable than 4-HBAEBT against thermal decomposition. Poly(aminobenzothiazole)s without phenolic substitutions have been

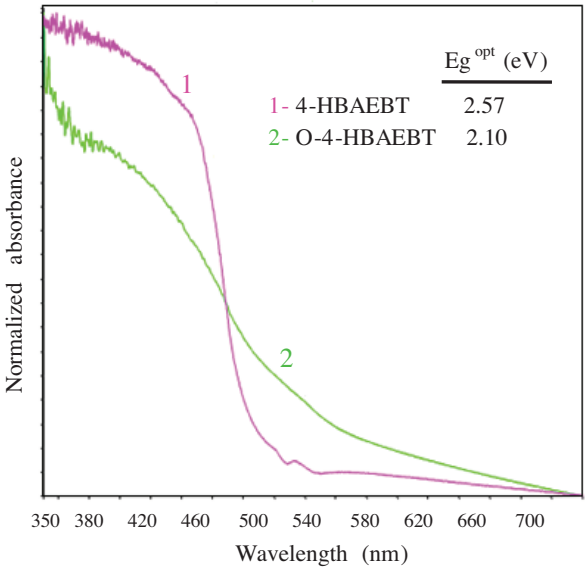

Figure 9. UV-Vis spectra of 4-HBAEBT (1) and the O-4-HBAEBT (2) in PMMA gel matrix.

previously found to thermally degrade at about 150–180 °C.[20,28] That is to say, the present oligomer, which is iminophenylene substituted oligo(benzothiazole), has higher thermal stability than the previously presented unsubstituted forms. O-4-HBAEBT has a low mass loss at the first step, but a great loss at the second. The first and second steps at ∼300 and 900 °C are characteristic for polyphenol species and these steps are attributed to depolymerization from C–C and C–O–C couplings.[29] The high mass loss at the second step indicates the high rate of C–O–C coupling, in agreement with the NMR results. The C–O–C/C–C coupling rate is calculated as ∼5/1, indicating 17% C–C coupling for O-4-HBAEBT, as in the literature.[29,30] The TG-DTA curves of a film sample of the oligomer in the PMMA matrix is given in Figure 10c and the results are summarized in Table 3. As compared with Figures 10b and 10c, the powder sample of O-4-HBAEBT is much more stable than that in the PMMA matrix. This is possibly because of the unstable components in the gel matrix. The film sample loses only 3% of its weight until 274 °C due to evaporation of adsorbed moisture, and starts to quickly decompose at this temperature. The film sample loses 87% of its weight in this fast decomposition step up to 350 °C. The other step is ranging to 770 °C and all sample weight is lost at this temperature.

DSC analysis of the oligomer is also carried out in order to determine the glass transition temperature (Tg) and endothermic/exothermic peak temperatures (Figure 11). The results are summarized in Table 3. The Tg temperature of the oligomer is found as 105 °C. The exothermic peak at 345 °C coincides with the first degradation step and indicates the exothermic depolymerization step of the oligomer. As a result of the thermal analysis, glassy transition of the synthesized oligomer occurs at about 105 °C, and then the oligomer starts to exothermically decompose above 293 °C with two particular degradation steps.

3. Conclusions

Oligo(azomethine-ether) with benzothiazole moieties was successfully synthesized in an organic medium. Fluorescence measurements showed that the oligomer had good emission characteristics. O-4-HBAEBT showed a solvatochromic PL effect. Its maximum emission value in DMF was 95 nm red shifted compared to that in $CHCl_3$. Additionally, O-4-HBAEBT was a green light emitter with relatively high QY in the PMMA matrix,

while the monomer emitted blue light with low QY in similar conditions. Accordingly, O-4-HBAEBT could be used as an alternative PLED for green color. The spectral and thermal findings showed a high rate of C–O–C coupling during the polymerization. The synthesized oligomer had quite high thermal stability while its average molecular weight was only $\sim$3200 g mol^{-1}. Cross linking caused the hydroxyl groups to greatly reduce in number. This was also confirmed by CV measurements by reducing the intensity of electro-active hydroxyl peaks. As a result, with its good solubility and thermal and optical properties, the synthesized oligomer might be applied practically in appliances.

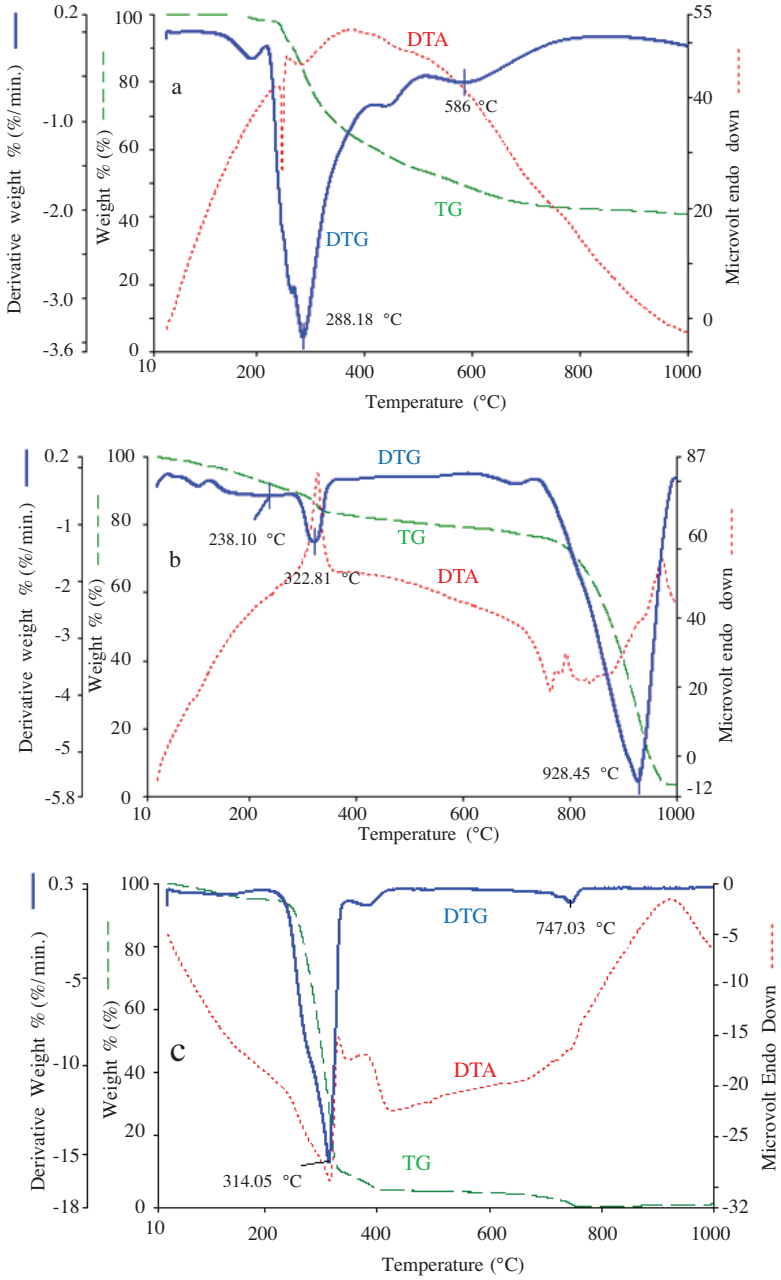

Figure 10. TG-DTA curves of 4-HBAEBT (a), O-4-HBAEBT (b) in powder samples and O-4-HBAEBT in PMMA matrix (c).

Table 3. Thermal analysis results of the synthesized compounds.

Compounds	TG-DTG								DSC		
	1st step			2nd step							
	[a]T_{on} (°C)	[b]T_{max} (°C)	[c]%	T_{max} (°C)	%	[d]T_{20} (°C)	[e]T_{50} (°C)	Char. at 1000 °C (%)	endo	exo	[f] Tg (°C)
[1]4-HBAEBT	249	288	44	586	13	301	610	43	-	-	-
[1]O-4-HBAEBT	293	323	14	928	73	703	883	5	-	345	115
[2]O-4-HBAEBT	274	315	87	749	10	280	305	0	-	-	-

[a]Degradation onset temp. [b]Maximum weight loss temp. [c]Weight loss percentage.
[d]20% weight loss temp. [e]50% weight loss temp. [f] Glass transition temp.
[1]Powder sample, [2]Film sample in PMMA matrix

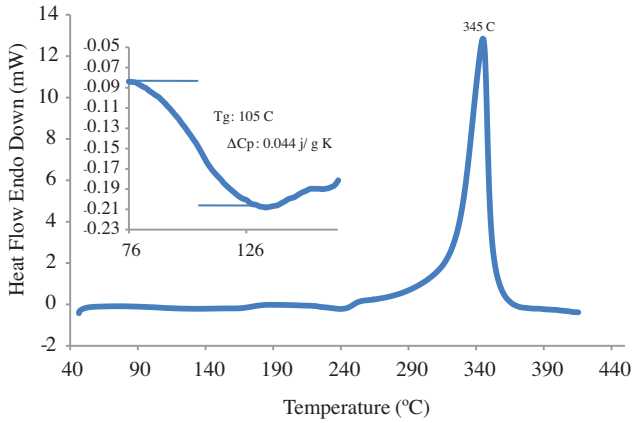

Figure 11. DSC curve of O-4-HBAEBT in powder form.

4. Experimental

4.1. Chemicals

2-Amino-6-ethoxybenzothiazole (EBT), 4-hydroxybenzaldehyde (4-HBA), poly(methylmetacrylate) (PMMA, M_n: 70,000 g mol^{-1}), propylene carbonate (PC), $LiClO_4$, $NaClO_4$, dimethylsulfoxide (DMSO), N,N-dimethylformamide (DMF), acetonitrile (MeCN), tetrahydrofurane (THF), methanol, ethanol, and chloroform were supplied by Merck Chemical Co. (Germany). Tetrabutylammoniumhexafluorophosphate ($TBAPF_6$) was supplied by Fluka, while 30% aqueous solution of sodium hypochlorite (NaOCl) was supplied by Paksoy Chemical Co. (Turkey).

4.2. Synthesis of the Schiff base monomer

The synthesis procedure is summarized in Scheme 3. The Schiff base monomer, 4-((6-ethoxybenzothiazol-2-ylimino)methyl) phenol (4-HBAEBT), was synthesized by condensation reaction of 4-hydroxybenzaldehyde (4-HBA) and 2-amino-6-ethoxybenzothiazole (EBT). The reaction was performed as follows: EBT (3.88 g, 0.02 mol) was placed into a 250-mL three-necked round-bottom flask fitted with a condenser, thermometer, and magnetic stirrer. Then 50 mL of methanol was added to the flask and the reaction mixture was heated up to 60 °C. A solution of 4-HBA (2.44 g, 0.02 mol) in 10 mL of methanol was added to the flask. The reaction was maintained for 3 h under reflux. Then the solvent was evaporated at room temperature. The obtained solid

was recrystallized from MeCN and dried in a vacuum desiccator (yield: 85%). The purity of 4-HBAEBT was checked by melting point (T_m) measurement. T_m was 220 °C and stable during melting.

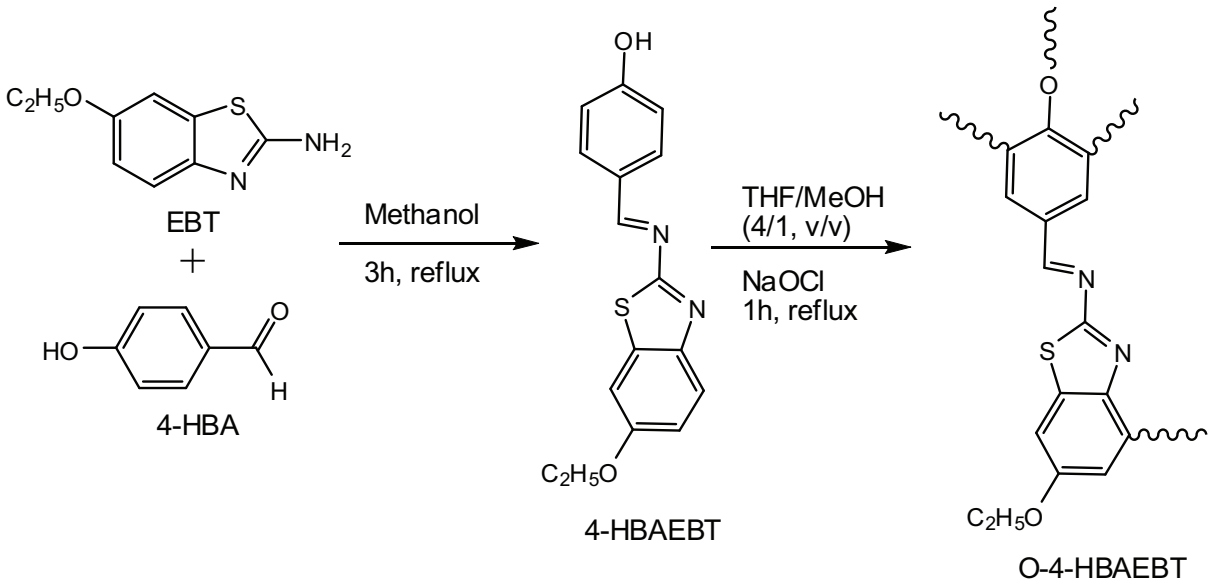

Scheme 3. Synthesis routes of 4-HBAEBT and O-4-HBAEBT.

4.3. Synthesis of the oligomer

The polymerization method is given in Scheme 3. The oligomer of 4-HBAEBT was synthesized in an organic solvent mixture (an optimized solvent system was determined as a result of various experiments) according to the following procedure: 0.3 g of 4-HBAEBT was placed into a 100-mL two-necked round-bottom flask fitted with a condenser and magnetic stirrer. A solvent mixture including 10 mL of THF and 40 mL of MeOH was added to the flask. The reaction mixture was heated up to boiling point and 1 mL of NaOCl solution (30% concentrated) was added to the solution as oxidant. The color of the medium was converted to brown by addition of the oxidant. The reaction was maintained for 1 h under reflux, and then the reaction mixture was concentrated by a rotary evaporator. The residual solution (∼5 mL) was transferred into a beaker and kept at room temperature for 2 days. The obtained black solid was washed with water (2 × 50 mL) and MeCN (3 × 50 mL) in order to remove inorganic salts and unreacted monomer, respectively. The obtained oligomer was filtered and dried in a vacuum oven at 80 °C for 24 h.

4.4. Preparation of the film materials in PMMA matrix

The PMMA gel matrix was prepared from $NaClO_4$:$LiClO_4$:MeCN:PMMA:PC in the ratio of 3:3:80:14:40 by weight as described in the literature[31] Homogeneous film surfaces of 4-HBAEBT and O-4-HBAEBT involving the PMMA gel matrix as extender were prepared on a transparent polyester plate using the following procedure: 0.5 g of the monomer and O-4-HBAEBT were separately dissolved in 40 mL of THF and added to 100-mL beakers. The mixtures were boiled for about 5 min in a fume hood and accordingly concentrated. Then 0.5 g of PMMA gel matrix was added to the solutions and the mixtures were vigorously stirred and evaporated to be about 10 mL in volume. The obtained homogeneous viscous mixtures were added to previously prepared polyester slices and spread. The materials were dried at room temperature for 5 days.

4.5. Characterization techniques

The solubility tests were carried out in different solvents using 1 mg of sample and 1 mL of solvent at 25 °C. The infrared spectra were measured by PerkinElmer FT-IR Spectrum one using a universal ATR sampling accessory (4000–650 cm^{-1}). ^1H NMR spectra (Bruker AC FT-NMR spectrometer operating at 400 MHz) were recorded using deuterated DMSO-d_6 as solvent at 25 °C. Tetramethylsilane was used as internal standard. Scanning electron microscopy (SEM) photographs of the oligomers were recorded using a Philips XL-305 FEG SEM instrument. Prior to the measurements, oligomer samples were dried in a vacuum oven at 70 °C for 24 h to remove the residual moisture. Gold/palladium coated thin films of the oligomer samples were used for SEM measurements. Melting point of the Schiff base monomer was measured by Electrothermal 9100 melting point measurement instrument. Thermal data were obtained using a PerkinElmer Diamond Thermal Analysis system. TG-DTA measurements were made between 20 and 1000 °C (in N_2, rate 10 °C/min). DSC analyses were carried out by using a PerkinElmer Pyris Sapphire DSC between 25 and 420 °C (in N_2, rate 10 °C/min). The number average molecular weight (M_n), weight average molecular weight (M_w), and polydispersity index (PDI) were determined by size exclusion chromatography (SEC) techniques of Shimadzu Co. For SEC investigations an SGX (100 Å and 7 nm diameter loading material) 3.3 mm i.d. × 300 mm column was used; eluent: DMF (0.4 mL/min), polystyrene standards. A refractive index detector (RID) was used to analyze the products at 55 °C.

4.6. Optical and electrochemical properties

Ultraviolet-visible (UV-Vis) spectra of compounds were measured by Analytikjena Specord 210 Plus. The solution state absorption spectra were recorded in methanol solutions. Measurements were carried out at 25 °C. The absorption spectra in the PMMA matrix were also measured upon the film surface. The optical band gaps (E_g^{opt}) were calculated from the absorption edges as in the literature,[32] by the following equation:

$$Eg^{opt} = 1242 \,/\, \lambda_{onset},$$

where λ_{onset} indicates the onset wavelength determined by the intersection of two tangents drawn on the absorption edge (shown in Figure 5).

A Shimadzu RF-5301PC spectrofluorophotometer was used for fluorescence measurements. Solution state photoluminescence (PL) spectra were obtained in $CHCl_3$ and DMF solutions. Solution concentrations were adjusted to 0.1 g L^{-1} for all measurements. Slit width was 5 nm in all measurements. Solid state PL characteristics were determined on the film surfaces in the PMMA matrix. Fluorescence quantum yields (QYs) of the solid state PL colors were determined using the comparative method as described in the literature.[20,33] Fluorescein solution in 0.1 M of aqueous NaOH was used as the standard.

CV measurements were carried out with a CHI 660 C Electrochemical Analyzer (CH Instruments, Bee Cave, TX, USA) at a potential scan rate of 20 mV/s. All the experiments were performed in a dry box filled with argon at room temperature. The electrochemical potential of Ag was calibrated with respect to the ferrocene/ferrocenium (Fc/Fc^+) couple. The half-wave potential ($E^{1/2}$) of (Fc/Fc^+) measured in MeCN solution of 0.1 M $TBAPF_6$ was 0.39 V with respect to Ag wire. The voltammetric measurements were carried out in a MeCN/DMSO mixture (v/v, 4/1). The HOMO–LUMO energy levels and electrochemical band gaps (E_g') were calculated from the oxidation and reduction peak potentials, using the following equations:[34]

E_{HOMO}: $-(4.39 + E_{ox})$

E_{LUMO}: $-(4.39 + E_{red})$

E'_g: $E_{LUMO} - E_{HOMO}$,

where E_{ox} and E_{red} are oxidation and reduction peak potentials, respectively.

References

1. Pron, A.; Rannou, P. *Prog. Polym. Sci.* **2002**, *27*, 135–190.
2. Waris, G.; Siddiqi, H. M.; Twyman, L. J.; Hussain, R.; Akhter, Z.; Butt, M. S. *Turk. J. Chem.* **2013**, *37*, 946–958.
3. Lee, B. R.; Kim, J. S.; Nam, Y. S.; Jeong, H. J.; Jeong, S. Y.; Lee, G. W.; Han, J. T.; Song, M. H. *J. Mater. Chem.* **2012**, *22*, 21481–21486.
4. Chuang, C. N.; Chuang, H. J.; Wang, Y. X.; Chen, S. H.; Huang, J. J.; Leung, M. K.; Hsieh, K. H. *Polymer* **2012**, *53*, 4983–4992.
5. Karasz, F. E.; Hu, B.; Yang, Z. *Turk. J. Chem.* **1997**, *21*, 1–5.
6. Deniz, T. K.; Apaydın, D. H.; Özelçağlayan, A. C.; Toppare, L. K.; Çırpan, A. *Turk. J. Chem.* **2013**, *37*, 538–546.
7. Takagi, S.; Makuta, S.; Veamatahau, A.; Otsuka, Y.; Tachibana, Y. *J. Mater. Chem.* **2012**, *22*, 22181–22189.
8. Bozkurt, A. *Turk. J. Chem.* **2002**, *26*, 663–668.
9. Benzarti-Ghedira, M.; Hrichi, H.; Jaballah, N.; Ben Chaabane, R.; Majdoub, M.; Ben Ouada, H. *Physica B* **2012**, *407*, 1051–1054.
10. Goncalves, V. C.; Balogh, D. T. *Sensor. Actuat. B-Chem.* **2012**, *162*, 307–312.
11. Lu, Y.; Li, X.; Wang, G. K.; Tang, W. *Biosens. Bioelectron.* **2013**, *39*, 231–235.
12. More, A. S.; Sane, P. S.; Patil, A. S.; Wadgaonkar, P. P. *Polym. Degrad. Stabil.* **2010**, *95*, 1727–1735.
13. Demir, H. O. *Polym. J.* **2012**, *44*, 699–705.
14. Kaya, İ.; Yıldırım, M. *J. Appl. Polym. Sci.* **2007**, *106*, 2282–2289.
15. Kaya, İ.; Aydın, A. *E-Polymers*, **2008**, *71*, 1.
16. Bilici, A.; Kaya, İ.; Yıldırım, M.; Dogan, F. *J. Mol. Catal. B-Enzym.* **2010**, *64*, 89–95.
17. Kaya, İ.; Yıldırım, M.; Kamacı, M. *Eur. Polym. J.* **2009**, *45*, 1586–1598.
18. Bilici, A.; Dogan, F.; Yıldırım, M.; Kaya, İ. *J. Phys. Chem. C* **2012**, *116*, 19934–19940.
19. Kaya, İ.; Yıldırım, M.; Aydın, A.; Şenol, D. *React. Funct. Polym.* **2010**, *70*, 815–826.
20. Yıldırım, M.; Kaya, İ. *Synthetic Met.* **2012**, *162*, 2443–2450.
21. Akgul, C.; Yıldırım, M. *J. Serb. Chem. Soc.* **2010**, *75*, 1203–1208.
22. Liu, C.; Wang, J. Y.; Lin, E. C.; Zong, L. S.; Jian, X. G. *Polym. Degrad. Stabil.* **2012**, *97*, 460–468.
23. Yang, J.; Yang, X. L.; Zou, Y. K.; Zhan, Y. Q.; Zhao, R.; Liu, X. B. *J. Appl. Polym. Sci.* **2012**, *126*, 1129–1135.
24. Kalamaras, I.; Daletou, M. K.; Neophytides, S. G.; Kallitsis, J. K. *J. Membrane Sci.* **2012**, *415*, 42–50.
25. Bilici, A.; Kaya, İ.; Yıldırım, M. *Eur. Polym. J.* **2011**, *47*, 1005–1017.
26. Topal, S. Z.; Yuksel, F.; Gurek, A. G.; Ertekin, K.; Yenigul, B.; Ahsen, V. *J. Photoch. Photobio. A* **2009**, *202*, 205–213.
27. Yigitsoy, B.; Varis, S.; Tanyeli, C.; Akhmedov, I. M.; Toppare, L. *Thin Solid Films* **2007**, *515*, 3898–3904.
28. Yıldırım, M.; Kaya, İ. *Synthetic Met.* **2012**, *162*, 834–842.
29. Peng, Y.; Liu, H. W.; Zhang, X. Y.; Li, Y. S.; Liu, S. Y. *J. Polym. Sci. Pol. Chem.* **2009**, *47*, 1627–1635.

30. Bilici, A.; Dogan, F.; Yıldırım, M.; Kaya, İ. *Mater. Chem. Phys.* **2013**, *140*, 66–74.

31. Cırpan, A.; Argun, A. A.; Grenier, C. R. G.; Reeves, B. D.; Reynolds, J. R. *J. Mater. Chem.* **2003**, *13*, 2422–2428.

32. Colladet, K.; Nicolas, M.; Goris, L.; Lutsen, L.; Vanderzande, D. *Thin Solid Films* **2004**, *451*, 7–11.

33. Williams, A. T. R.; Winfield, S. A.; Miller, J. N. *Analyst* **1983**, *108*, 1067–1071.

34. Cervini, R.; Li, X. C.; Spencer, G. W. C.; Holmes, A. B.; Moratti, S. C.; Friend, R. H. *Synthetic Met.* **1997**, *84*, 359–360.